For correspondence
wellenk@upenn.edu

Co peting interest **See page 16**

Funding **See page 16**

Received **01 September 2020**
Accepted **02 July 2021**
Published **30 November 2021**

Reviewing editor **Lydia WS Finley, Memorial Sloan Kettering Cancer Center, United States**

HBP flux and are upregulated in malignant tissue (Lau et al., 2007), and targeting the relevant Golgi GlcNAc transferase enzymes can limit tumor growth and metastasis in vivo (Granovsky et al., 2000; Li et al., 2008; Zhou et al., 2011). Thus, improved understanding of the regulation of the HBP in cancer could point towards novel therapeutic strategies.

Pancreatic ductal adenocarcinoma (PDA) is a deadly disease with a 5 year survival rate of 9% and a rising number of annual deaths (Rahib et al., 2014) (ACS Cancer Facts and Figures 2019, NIH SEER report 2019). Mutations in *KRAS* occur in nearly all cases of human PDA and drive extensive metabolic reprogramming in cancer cells. Enhanced flux into the HBP was identified as a primary metabolic feature mediated by mutant KRAS in PDA cells (Ying et al., 2012). Hypoxia, a salient characteristic of the tumor microenvironment (Lyssiotis and Kimmelman, 2017), was shown to further promote expression of glycolysis and HBP genes in pancreatic cancer cells (Guillaumond et al., 2013). Notably, the glutamine analog 6-diazo-5-oxo-L-norleucine (DON), which inhibited the HBP, suppressed PDA metastasis, and sensitized PDA tumors to anti-PD1 therapy (Sharma et al., 2020). DON has also been reported to sensitize PDA cells to the chemotherapeutic gemcitabine in vitro (Chen et al., 2017). Additionally, a recently developed inhibitor targeting the HBP enzyme phosphoacetylglucosamine mutase 3 (PGM3) enhances gemcitabine-mediated reduction of xenograft tumor growth in vivo (Ricciardiello et al., 2020). Thus, the HBP may represent a therapeutic target in PDA, although the regulation of UDP-GlcNAc synthesis and the optimal strategies to target this

question of how nutrient deprivation impacts the synthesis of UDP-GlcNAc and its utilization for glycosylation. Understanding how PDA cells regulate these processes under nutrient limitation could identify therapeutic vulnerabilities. In this study, we investigated the impact of nutrient deprivation on the HBP and glycosylation in PDA cells, identifying a key role for hexosamine salvage through the enzyme N-acetylglucosamine kinase (NAGK) in PDA tumor growth.

Results

Tetra-antennary N-glycans and O-GlcNAcylation are minimally impacted by nutrient limitation in pancreatic cancer cells

To examine the effects of nutrient deprivation on glycosylation, we cultured cells under glucose or glutamine limitation and examined O-GlcNAc levels and cell surface phytohemagglutinin-L (L-PHA) binding, a readout of N-acetylglucosaminyltransferase 5 (MGAT5)-mediated cell surface N-glycans (Figure 1—figure supplement 1A,B), which are highly sensitive to UDP-GlcNAc availability (Lau et al., 2007). We focused on glucose and glutamine because of their requirement to initiate the HBP (Figure 1A). First, as a positive control, we examined HCT-116 and SW480 colon cancer cells, previously documented to have glucose-responsive O-GlcNAcylation (Park et al., 2010; Steenackers et al., 2016), which we also confirmed in HCT-116 cells (Figure 1B). Indeed, L-PHA binding was suppressed by glucose restriction in SW480 cells and by glutamine restriction in both colon cancer cell lines (Figure 1C). Next, to test whether glycans were sensitive to nutrient restriction in PDA cells, we examined L-PHA binding and O-GlcNAc levels under nutrient deprivation conditions in a panel of human PDA cell lines, including PANC-1, MIA PaCa-2, AsPC-1, and HPAC. Across these cell lines, no consistent changes in L-PHA binding were observed under glucose or glutamine limitation (Figure 1D,E, Figure 1—figure supplement 1C

Figure 1. MGAT5-dependent N-glycans are minimally impacted by glucose or glutamine deprivation in PDA cells. (**A**) Overview of the hexosamine biosynthesis pathway (HBP). (**B**) O-GlcNAc levels in HCT-116 cells in high and low nutrients; cells were incubated in indicated concentrations of glucose and glutamine for 48 hr. (**C**) Phytohemagglutinin-L (L-PHA) binding in colon cancer cells. Cells were incubated in the indicated concentrations of glucose (left) or glutamine (right) for 48 hr and then analyzed by flow cytometry. Graph shows mean fluorescence intensity (MFI) relative to control condition. Statistical significance was calculated by unpaired t-test. (**D, E**) L-PHA binding in pancreatic ductal adenocarcinoma (PDA) cells in low nutrients. Cells were incubated in the indicated concentrations of glucose (**D**) or glutamine (**E**) for 48 hr and then analyzed by flow cytometry. Statistical significance was calculated by one-way ANOVA. (**F**) O-GlcNAc levels in PDA cells in high and low nutrients. Cells were incubated in the indicated

Figure 1 continued on next page

GlcNAc (Figure 2B

Figure 2. De novo UDP-GlcNAc synthesis is suppressed upon glutamine deprivation. (**A**) Metabolite measurements in PANC-1 cells after culture for 48 hr in 0.05 mM glutamine. Quantification is normalized to 4 mM glutamine condition. Statistical significance was calculated by unpaired t-test. Mean ± SEM of five biological replicates is represented. (**B**) Overview of the GlcNAc salvage pathway feeding into the HBP. GlcNAc scavenged from O-GlcNAc removal or lysosomal breakdown of glycans can be phosphorylated by NAGK and used to regenerate UDP-GlcNAc. (**C**) Overview of the incorporation of ^{13}C glucose into UDP-GlcNAc. Different parts of the molecule can be labeled from glucose-derived subunits; thus, isotopologs up to M+16 can be derived from glucose. (**D**) ^{13}C glucose tracing into F-6-P, GlcNAc-P, and UDP-GlcNAc in indicated glutamine concentrations. % labeled GlcN indicates sum of M+6 and M+8 isotopologs for GlcNAc-P and sum of M+6, M+8, M+11, and M+13 for UDP-GlcNAc. % labeled Ribose indicates

Figure 2 continued on next page

(Ryczko et al., 2016; Wellen et al., 2010). Endogenous sources of GlcNAc may include removal of O-GlcNAc protein modifications or breakdown of glycoconjugates and extracellular matrix components. Notably, intracellular levels of GlcNAc increase upon glutamine restriction (Figure 3A). Yet, the significance of GlcNAc salvage to maintenance of UDP-GlcNAc pools has been little studied, and the proportion of UDP-GlcNAc generated via the NAGK-dependent salvage pathway is unknown.

NAGK mRNA expression increased in PDA cell lines in low glutamine conditions and in some cell lines also in low glucose (Figure 2—figure supplement 3A,B). *GFPT1* expression was also induced in both low glucose conditions, consistent with a prior report (Moloughney et al., 2016), and in low glutamine conditions (Figure 2—figure supplement 3A), even though de novo synthesis is suppressed when glutamine is limited. Protein levels of NAGK did not increase in concordance with mRNA at these time points, however, although a mobility shift potentially indicative of post-translational modification was apparent when protein lysates were run on a gel using a large electrophoresis system (see Materials and methods; Figure 2—figure supplement 3C,D). Removal of the phosphatase inhibitor Na_3VO_4 from the sample buffer prevented the mobility shift, suggesting that NAGK may be phosphorylated on one or more residues in low glutamine conditions (Figure 2—figure supplement 3D). Taken together, these data indicate that under low glutamine conditions, GlcNAc availability for salvage increases and the salvage enzyme NAGK is subject to regulation.

These findings prompted us to investigate the role of NAGK in UDP-GlcNAc synthesis in PDA cells. We functionally examined the role of NAGK in PDA cell lines by using CRISPR-Cas9 gene editing to generate NAGK knockout (KO) PANC-1 and MiaPaCa-2 clonal cell lines (Figure 3—figure supplement 1A, B). N-[1,2-$^{13}C_2$]acetyl-D-glucosamine (^{13}C GlcNAc) was efficiently salvaged in control cells, and this was suppressed by NAGK deletion, as evidenced by reduced fractional labeling of GlcNAc-P and UDP-GlcNAc (Figure 3B). Since we did not observe any residual protein expression, we hypothesized that the N-acetylgalactosamine (GalNAc) salvage enzyme GalNAc kinase (GALK2) might be responsible for the remaining GlcNAc salvage in the absence of NAGK. Indeed, silencing of GALK2 further suppressed incorporation of ^{13}C GlcNAc into GlcNAc-P and UDP-GlcNAc in the NAGK KO cells (Figure 3—figure supplement 1C).

We hypothesized that knockout cells would conversely conduct increased de novo UDP-GlcNAc synthesis. To test this, we incubated cells with [U-^{13}C]-glucose and examined incorporation into GlcNAc-P and UDP-GlcNAc. Indeed, in the absence of NAGK, we observed increased glucose-dependent fractional labeling of the glucosamine ring of UDP-GlcNAc and GlcNAc-P, but not the ribose component of UDP-GlcNAc (Figure 3C,D, Figure 3—figure supplement 1D,E). This effect was also observed with knockdown of NAGK by shRNA, though to a lesser extent (Figure 3—figure supplement 2A,B). Incorporation of glucose into F-6-P did not change (Figure 3C), and the proportion of UDP-GlcNAc containing an M+5 ribose ring was also unchanged in knockout cells (Figure 3D), as expected. Thus, when NAGK is deleted and GlcNAc salvage is suppressed, de novo hexosamine synthesis increases.

We next assessed changes in the levels of hexosamine intermediates in control and NAGK KO cell lines. In PANC-1 KO cells in 4 mM glutamine, GlcN-P increased significantly, consistent with increased de novo synthesis in the absence of NAGK (Figure 3E). GlcNAc-P was modestly reduced in KO cells, though UDP-GlcNAc levels were maintained (Figure 3E). In MIA PaCa-2 cells, GlcNAc-P

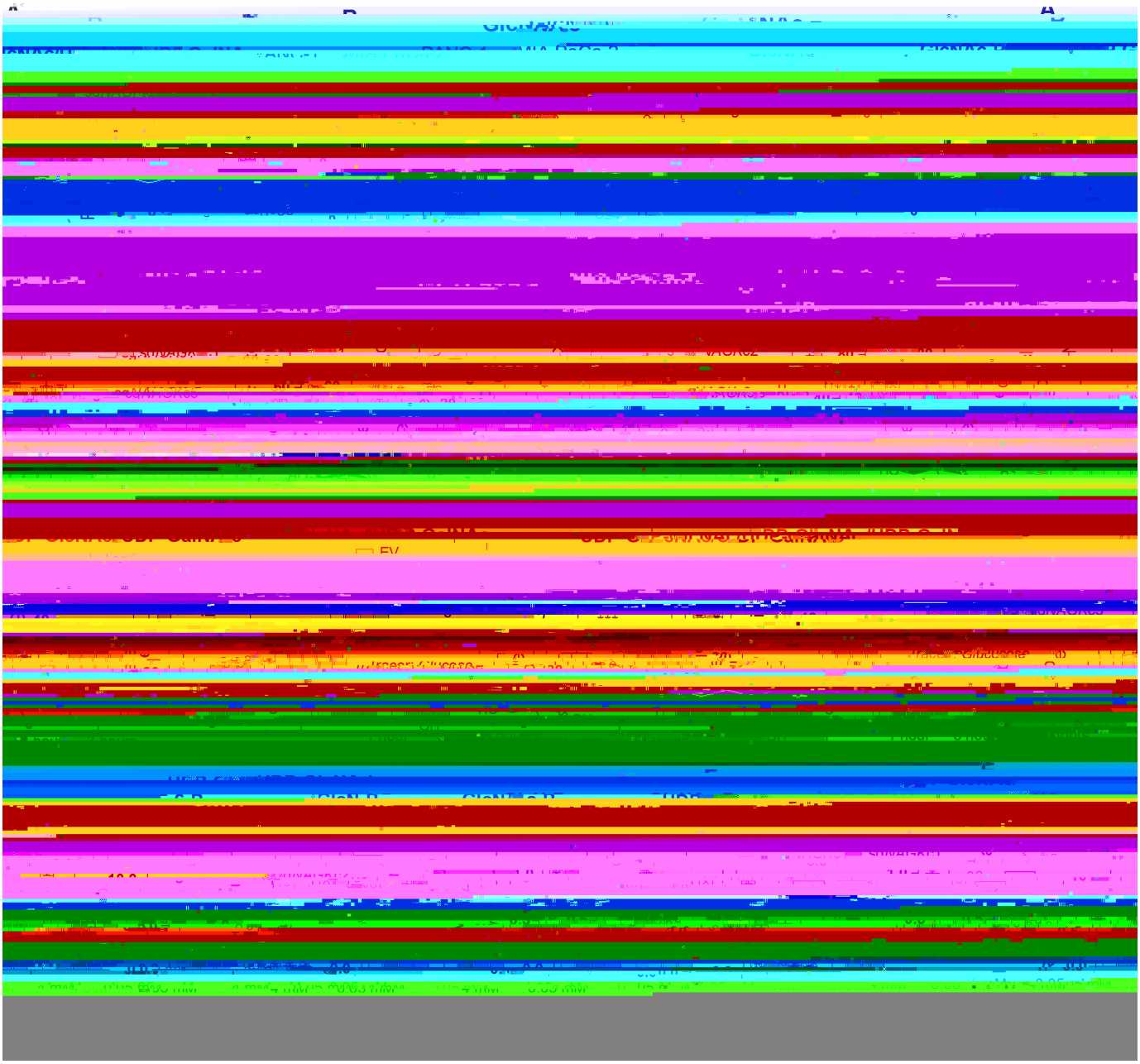

Figure 3. GlcNAc salvage feeds UDP-GlcNAc pools in pancreatic cancer cells. (**A**) Measurement of GlcNAc in PANC-1 and MIA PaCa-2 cells after incubation in the indicated concentrations of glutamine for 24 and 48 hr. Mean ±

to die quickly in low glutamine, which will be discussed further in the next section. GlcN-P decreased in control and KO cells, consistent with reduced de novo hexosamine synthesis (Figure 3E). GlcNAc-P levels decreased in low glutamine in control cells and decreased further in cells lacking NAGK, consistent with contributions from both de novo synthesis and salvage (Figure 3E). Reciprocally, GlcNAc abundance was elevated upon glutamine limitation in both control and NAGK KO cells (Figure 3E). UDP-GlcNAc abundance was modestly reduced in NAGK KO cells relative to controls

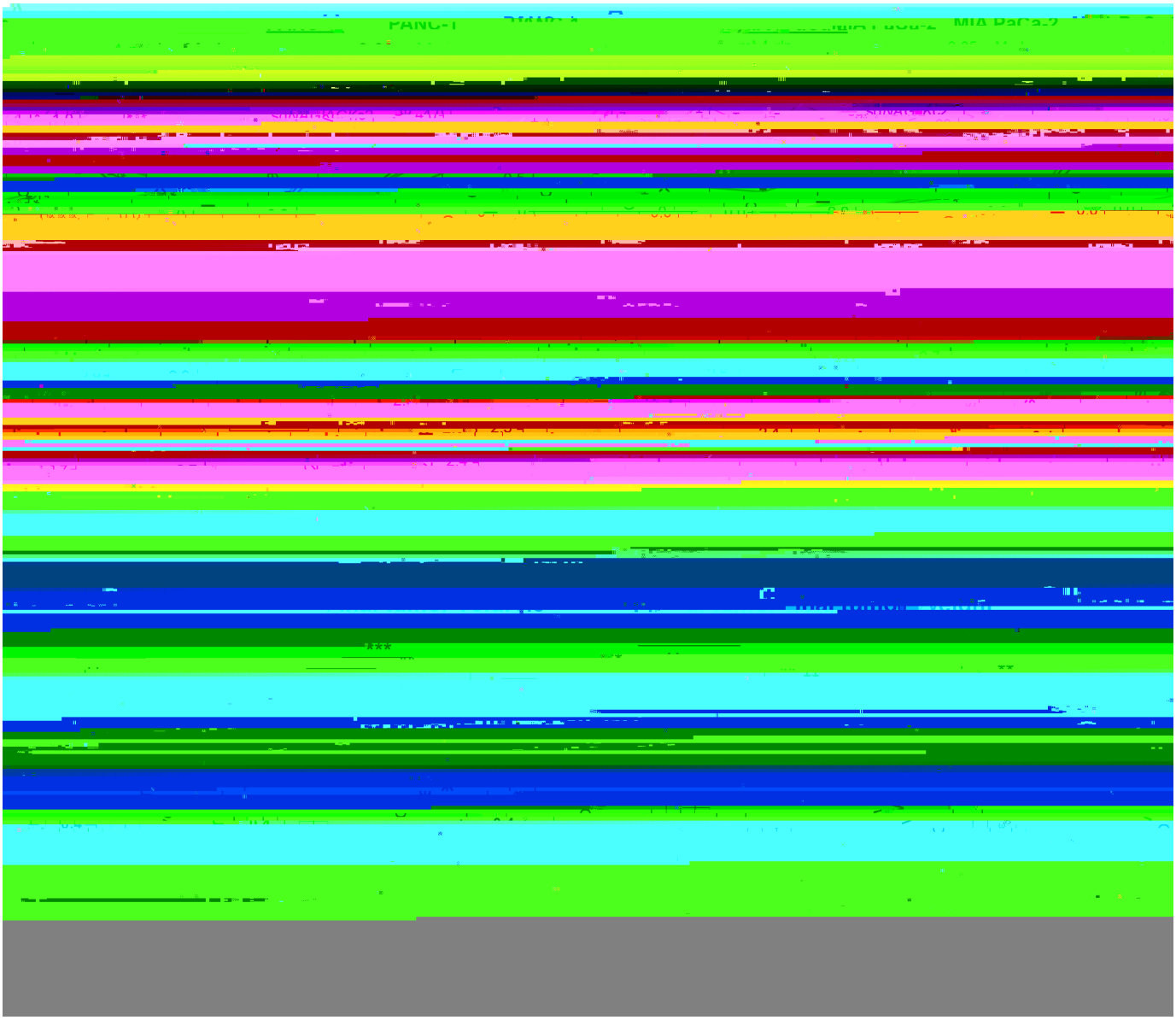

Figure 4. NAGK expression is increased in human PDA tumors and NAGK knockout reduces tumor growth in vivo. (**A**) 2D proliferation assay by cell count in PANC-1 and MIA PaCa-2 NAGK knockout cells. Mean ± SEM of three technical replicates is represented. Statistical significance was calculated using one-way ANOVA at each time point. (**B**) Gene expression data for NAGK, GFPT1, PGM3, and UAP1 in human PDA tumors compared with matched normal tissue. Statistical analysis was conducted by one-way ANOVA, and level of significance was defined as p□0.01. (**C**) Final tumor volume and (**D**) final tumor weight of subcutaneous tumors generated from PANC-1 NAGK knockout cells in vivo. Cells were injected into the right flank of NCr nude mice, and tumor volume was calculated from caliper measurements. Statistical significance was calculated by one-way ANOVA comparing each mean to the EV control mean. Mean ± SEM of biological replicates is represented (n = 8 each group). *p □ 0.05; **p □ 0.01; ***p □ 0.001.
The online version of this article includes the following figure supplement(s) for figure 4:

Figure supplement 1. NAGK knockout tumors show increased L-PHA binding.

Discussion

In this study, we identify a key role for NAGK in salvaging GlcNAc for UDP-GlcNAc synthesis in PDA cells. We show that glutamine deprivation suppresses de novo hexosamine biosynthesis, which is reciprocally increased upon NAGK deletion. Glutamine deprivation also results in increased availability of GlcNAc for salvage. *NAGK* expression is elevated in human PDA tumors, and NAGK deficiency suppresses GlcNAc salvage in cells and tumor growth in mice.

This work raises several key questions for future investigation. First, the sources of GlcNAc salvaged by NAGK remain to be fully elucidated. GlcNAc may be derived from recycling of GlcNAc fol-

Continued

Reagent type (species) or resource	Designation	Source or reference	Identifiers	Additional information
Sequence-based reagent	**HPRT** reverse	This paper	RT-qPCR primers	CCCATCTCCTT CATGACATCT
Sequence-based reagent	**RPL19** forward	This paper	RT-qPCR primers	CAAGAAGGAG GAGATCATCAAG
Sequence-based reagent	**RPL19** reverse	This paper	RT-qPCR primers	ATCACAGAGGCC AGTATGTA
Sequence-based reagent	sg**MGAT5** mouse forward	**Doench et al., 2016**	CRISPR deletion primers	CACCGGCTGTCATG ACACCAGCGTA
Sequence-based reagent	sg**MGAT5** mouse reverse	**Doench et al., 2016**	CRISPR deletion primers	AAACTACGCTGGTGT CATGACAGCC
Sequence-based reagent	sg**NAGK**#1 forward	**Doench et al., 2016**	CRISPR deletion primers	CACCGTTGAC GTAGCCGATATCATG
Sequence-based reagent	sg**NAGK**#1 reverse	**Doench et al., 2016**	CRISPR deletion primers	AAACCATGATAT CGGCTACGTCAAC
Sequence-based reagent	sg**NAGK**#2 forward	**Doench et al., 2016**	CRISPR deletion primers	CACCGTGCTTG GTGTGCGATCCAGT
Sequence-based reagent	sg**NAGK**#2 reverse	**Doench et al., 2016**	CRISPR deletion primers	AAACACTGGA TCGCACACCAAGCAC
Sequence-based reagent	sg**NAGK**#3 forward	**Doench et al., 2016**	CRISPR deletion primers	- CACCGCTNAGK sg**NAGK** based reagent

different sgRNAs, four in PANC-1 cells and three in MIA PaCa-2 cells, were chosen for use in the

Samples were prepared according to Guo et al., 2016b. Briefly, cells were put on ice and washed 3□ with PBS. Then, 1 mL of ice cold 80% methanol was added to the plate, and cells were scraped into solvent and transferred to a 1.5 mL tube. For quantitation experiments, internal standard containing a mix of ^{13}C labeled metabolites was added at this time. Samples were then sonicated and spun down, and the supernatants were dried down under nitrogen. The dried samples were then resuspended in 100 μL of 5% sulfosalicylic acid and analyzed by liquid chromatography–high-resolution mass spectrometry as reported (Guo et al., 2016b) with the only modification that the LC was coupled to a Q Exactive-HF with a heated ESI source operating in negative-ion mode alternating full scan and MS/MS modes. The [M-H]□

cervical dislocation. Tumors were removed, weighed, cut into pieces for analysis, and frozen. All animal experiments were approved by the University of Pennsylvania and the Institutional Animal Care and Use Committee (IACUC).

Acknowledgements

Funding sources: This work was supported by R01CA174761 and R01CA228339 to KEW. This work was also funded in part under a grant with the Pennsylvania Department of Health to KEW and IAB. The Department specifically disclaims responsibility for any analyses, interpretations, or conclusions. IAB acknowledges support of NIH Grants P30ES013508 and P30CA016520. JB acknowledges support of NIH Grant R01CA046595. SLC received support from T32CA115299 and F31CA217070, as well as from a Patel Family Scholar Award. HA was supported by post-doctoral fellowship K00CA212455. TT is supported by the National Cancer Institute through pre-doctoral fellowship F31CA243294 and acknowledges the Blavatnik Family for a predoctoral fellowship. LI is supported by T32 GM-07229 and T32 CA115299. ST is supported by the American Diabetes Association through post-doctoral fellowship 1–18-PDF-144. Funding sources were not involved in study design, data collection and interpretation, or the decision to submit the work for publication.

Additional information

Co peting interests

Ian A Blair: IAB is a founder of Proteoform Bio and a paid consultant for Calico, Chimerix, PTC Therapeutics, Takeda Pharmaceuticals, and Vivo Capital. The other authors declare that no competing interests exist.

Funding

Funder	Grant reference number	Author
National Cancer Institute	R01CA174761	Kathryn E Wellen
National Cancer Institute	R01CA228339	Kathryn E Wellen
Pennsylvania Department of Health		Ian A Blair Kathryn E Wellen
National Institute for Environmental Studies	P30ES013508	Ian A Blair
National Cancer Institute	(from)-68rf-331.301(114((u628)-536al)-327.2a)-332.1327.8	

Nationa9(Institu221.1598.95742Td[(~~Ian)-332.459(A)-330.171(Blair)~~]TJT*[(~~Kathryn)-32)~~]TJT*–
Aertm1927hn1.601(c53.14[(Ka6017uuEPl1ent)-334.156(of)]TJ7itut)13.0995(e)-33Sydney0.171(B8319mpbe17uu8111)-3*[(Kn)-322.59ntaIzzoKathryn E Wellen

Engle DD, Tiriac H, Rivera KD, Pommier A, Whalen S, Oni TE, Alagesan B, Lee EJ, Yao MA, Lucito MS, Spielman B, Da Silva B, Schoepfer C, Wright K, Creighton B, Afinowicz L, Yu KH, Grützmann R, Aust D, Gimotty PA, et al.

Wyant GA, **Abu-Remaileh M**, **Frenkel EM**, **Laqtom NN**, **Dharamdasani V**, **Lewis CA**, **Chan SH**, **Heinze I**, **Ori A**, **Sabatini DM. 2018. NUFIP1 is a ribosome receptor for starvation-induced ribophagy.** *Science* **360:751–758. DOI: https://doi.org/10.1126/science.aar2663, PMID: 29700228**

Ying H, **Kimmelman AC**, **Lyssiotis CA**, **Hua S**, **Chu GC**, **Fletcher-Sananikone E**, **Locasale JW**, **Son J**, **Zhang H**, **Coloff JL**, **Yan H**, **Wang W**, **Chen S**, **Viale A**, **Zheng H**, **Paik JH**, **Lim C**, **Guimaraes AR**, **Martin ES**, **Chang J**, **et al. 2012. Oncogenic kras maintains pancreatic tumors through regulation of anabolic glucose metabolism.** *Cell* **149:656–670. DOI: https://doi.org/10.1016/j.cell.2012.01.058, PMID: 22541435**

Zhou X, **Chen H**, **Wang Q**, **Zhang L**, **Zhao J. 2011. Knockdown of Mgat5 inhibits CD133+ human pulmonary adenocarcinoma cell growth in vitro and in vivo.** *Clin Exp Invest Active Med Chin* **34:155–162. DOI: https://doi.org/10.25011/cim.v34i3.15188, PMID: 21631992**